



## Effect of deformation, particle-hole and particle-particle interaction on Gamow-Teller transitions of $^{76}\text{Ge}$

Şadiye ÇAKMAK 

Program of Medical Monitoring Techniques, Osmangazi University, Eskişehir / TURKEY

### Abstract

Gamow-Teller (GT) transitions for  $^{76}\text{Ge}$  using QRPA methods in this article are calculated, which play an essential role in the supernovae. Three different QRPA models are used to calculate the GT strength distributions. QRPA models are namely single quasi-particle (sqp), Pyatov Method (PM) and the Schematic Model (SM). Gamow-Teller distribution,  $\Sigma B(\text{GT})$ , the centroid of energy, the width of energy and ISR are calculated by using these models. The effect of particle-particle interaction on spherical nuclei and deformed nuclei on Gamow-Teller transitions is wanted to show in this paper. Deformed Woods-Saxon potential is used in calculations of Single-particle energies and wave functions. The results are also compared with previous theoretical calculations and measured strength distributions wherever available. It is expected that the current study of GT features would be helpful and may guide to a better knowledge of the Pre-supernova progression of massive stars.

### Article info

#### History:

Received:12.01.2020

Accepted:12.06.2020

#### Keywords:

Gamow Teller Distribution, Germanium Isotope, Centroid of Energy, Width of Energy,  $\beta$ -decay and Electron Capture.

## 1. Introduction

It is known that nuclear beta decay and electron capture are the most important weak interaction processes to understand nuclear structure and mechanisms of astrophysical events. From the astrophysical point of view, these processes are of great importance in the calculations of supernova formation and the understanding of stages of stellar evolution. For example, they directly affect lepton to baryon ration  $Y_e$  and entropy at the Pre-supernova stage. It is known that Fermi and Gamow-Teller transitions feel their dominant characters in weak interactions in Pre-supernova stars [1-4]. Especially, in nucleus synthesis and stellar core collapse of massive stars, GT transitions are seen dominantly.

The Schrodinger equation of a multi-particle system couldn't be solved mathematically. The appropriate model is used in these cases. One of the widely used models in nuclear physics is the layer model. According to this model, each particle constituting a multi-particle system is thought to move at a common self-harmonized potential of other particles. In this study, it is considered that the particles act in a self-harmonized potential in our model. The local static potential (Woods-Saxon (WS) potential) is used as the self-harmonized potential in the model we use in this work. When the isovector vibrations in the nuclei are examined, appropriate multipole-multipole effective interaction is added to the mean field potential. Each added effective interaction includes one or more free parameters. The parameters are adjusted using the measured results. In Pyatov's method, this parameter is selected so that corrupted symmetries are restored. There is one difference in the application of the Pyatov method to Gamow-Teller transitions from that of other processes. In case of problems related to the Giant Dipole Resonance (GDR), Magnetic Dipole Resonance (MDR) and Isobar Analogue Resonance (IAR) processes, the disturbed symmetry of the Hamilton operator's core is restored. So in this case, the distorted commutation condition between the actual Hamilton operator and the GT operator is restored [5]. The Pyatov method [5] has been applied to different problems by different scientists. In addition, studies on the Pyatov method have been increasing in the last decade. Civitarese et al. were applied this method to isospin-dependent Hamiltonian written in quasi-particle space [6]. This method was also used by Magierski and Wyss [7]. Kuliev et al. used the Pyatov method to investigate scissors mode in deformation cores [8], Selam et al. used the Pyatov method to investigate the GTR properties in spherical nuclei and the isospin mixture in the ground state [9, 10, 11]. Necla studied charge Exchange collective excitations in odd mass nuclei by using Pyatov method [12].

\*Corresponding author. Email address: scakmak@ogu.edu.tr

There have been various experimental studies on Gamow-Teller  $\beta$  strength distributions via ( $d, ^2\text{He}$ )[13], ( $t, ^3\text{He}$ )[13], ( $^3\text{He}, t$ ) [14, 15], ( $n, p$ )[16] and ( $p, n$ ) [17] charge-exchange reactions. Data show that total GT strength is quenched and fragmented over many final states in the daughter nucleus. The data also show a misplacement in the GT centroid adopted in the parameterizations of Ref.[1]. There have been theoretical efforts to improve this discrepancy. In theoretical calculations, Large scale Shell Model [13-15,18-21], proton-neutron quasi-particle random phase approximation (pnQRPA) [3, 22, 23, 24], Shell Model Monte Carlo method [18, 19, 20, 22], HF+BCS (Hartree-Fock+Bardeen-Cooper-Schrieffer) and HF+BCS+QRPA [22] were used. The main focus of these efforts is on GT strength distributions of nuclei in germanium-regime. Especially,  $^{76}\text{Ge}$  is of particular astrophysical interest, and this has been the object of numerous theoretical studies [25-28]. This nucleus is related to each other through a well-known two- and zero-neutrino double beta ( $2\nu 2\beta$  and  $0\nu 2\beta$ ) decay mode [25]. That is why many papers have been focused on the study of those decays during the last decades [25]. In 1989, Madey and collaborators [29] studied the excitation-energy distributions of transition strength to  $1^+$  states excited via the ( $p, n$ ) reaction at 134.4 MeV on targets of  $^{76}\text{Ge}$  (along with two heavy isotopes of Te) for excitation energies up to 25 MeV. Sarriguren et al. studied the ground state and  $\beta$ -decay properties of exotic nuclei using a deformed self-consistent HF+BCS+QRPA (Hartree-Fock+Bardeen-Cooper-Schrieffer+Quasi-particle Random Phase Approximation) calculation with density dependent effective interactions of Skyrme type [30]. Sarriguren et al. extended those calculations to the study of the dependence on the deformation of the single  $\beta$  branches that build up the double  $\beta$  process. They concentrated on the double  $\beta$  decay of  $^{76}\text{Ge}$  and  $\beta^-$  Gamow-Teller (GT) transitions to the intermediate nucleus [26]. Recently Ha and Cheoun used a deformed quasi-particle random phase approximation (DQRPA) using the Brueckner G-matrix based on the CD Bonn potential to calculate ground-state GT strength distributions of  $^{76}\text{Ge}$  [27]. Jameel et al. used deformed pn-QRPA model with schematic separable interaction to calculate ground- and excited-states GT. transitions for  $^{76}\text{Ge}$  [28]. However, the excited state requires further results to calculate the GT strength distribution. In this study, Pyatov method and schematic model are used to calculate ground state  $\beta$ -decay rates for  $^{76}\text{Ge}$  and also results of single quasi-particle which is the basis of PM and SM are given. Several calculations regarding the deformation effects on the GT strength distributions have been reported in the past [26, 30]. In this paper, it is presented in detail how the deformation, particle-hole and particle-particle parameters affect single-particle states, and GT transitions in  $^{76}\text{Ge}$ , whose excited states are believed to be deformed by the E2 transition data [31]. The deformation effect was known as another important factor for estimating the decay rate [32, 33]. Actually, the ground states of  $^{76}\text{Ge}$  are known to be almost spherical. Because there is no clear evidence for the existence of rotational bands and also my results will show that GT  $1^+$  distributions results for spherical nuclei is closer to measured results than the corresponding results for deformed nuclei (see section 3).

In the next section, brief and necessary theoretical formalism is presented for spherical and deformed nuclei. GT-strength distributions results of germanium isotope with previous theoretical and measured results are compared and also GT. results with different deformation, particle-hole interaction and particle-particle interaction parameters are compared in the third section. The centroid and the width of calculated GT distributions are calculated and compared in this section. This study is summarized and conclusions are presented in the last section.

## 2. Theoretical Formalism

A brief summary of the necessary formalism for the three models used in this work is presented in this section. A system of nucleons in an axially symmetry average field interacting via pairing and spin-spin interactions with a charge-exchange. The Hamiltonian of the schematic model (SM) in quasi-particle representation is given by

$$H_{SM} = H_{SQP} + h_{ph} + h_{pp} \quad (1)$$

where  $HSQP$  is the single quasi-particle Hamiltonian and described by:

$$H_{SQP} = \sum_{s,\tau,\rho} E_s(\tau) \alpha_{s\rho}^\dagger \alpha_{s\rho}, \quad \tau = n, p \quad (2)$$

where  $E_s(\tau)$  is the single quasi-particle energy of nucleons,  $\alpha_{s\rho}^\dagger$  ( $\alpha_{s\rho}$ ) is the quasi-particle creation (annihilation) operator.  $h_{GT}^{ph}$  and  $h_{GT}^{pp}$  are the GT effective interactions in the particle-hole and particle-particle channels, respectively, and given as

$$\begin{aligned} h_{ph}^{GT} &= 2\mathcal{X}_{GT}^{ph} \sum_{\mu} \beta_{\mu}^{+} \beta_{\mu}^{-} \\ h_{pp}^{GT} &= -2\mathcal{X}_{GT}^{pp} \sum_{\mu} P_{\mu}^{+} P_{\mu}^{-}, \quad \mu = 0, \pm 1; \end{aligned} \quad (3)$$

With

$$\begin{aligned} \beta_{\mu}^{+} &= \sum_{n,p,\rho,\rho'} \langle n\rho | \sigma_{\mu} + (-1)^{\mu} \sigma_{-\mu} | p\rho' \rangle a_{np}^{\dagger} a_{p\rho'}, \quad \beta_{\mu}^{-} = (\beta_{\mu}^{+})^{\dagger} \\ P_{\mu}^{+} &= \sum_{n,p,\rho,\rho'} \langle n\rho | \sigma_{\mu} + (-1)^{\mu} \sigma_{-\mu} | p\rho' \rangle a_{np}^{\dagger} a_{pp'}^{\dagger}, \quad P_{\mu}^{-} = (P_{\mu}^{+})^{\dagger} \end{aligned} \quad (4)$$

where  $a_{np}^{\dagger}$  ( $a_{p\rho'}$ ) is the nucleon creation (annihilation) operator,  $\sigma_{\mu}$  is the spherical component of the Pauli operator. In the quasi-particle representation, the  $\beta_{\mu}^{\pm}$  and  $P_{\mu}^{\pm}$  operators are introduced as:

$$\begin{aligned} \beta_{\mu}^{+} &= \sum_{n,p} \left[ \frac{1}{\sqrt{2}} (\overline{d_{np}} D_{np}^{\dagger} + d_{np} D_{np}) + (\overline{b_{np}} C_{np}^{\dagger} - b_{np} C_{np}) \right] \\ P_{\mu}^{+} &= \sum_{n,p} \left[ \frac{1}{\sqrt{2}} (b_{np} D_{np}^{\dagger} - \overline{b_{np}} D_{np}) + (d_{np} C_{np}^{\dagger} + \overline{d_{np}} C_{np}) \right] \end{aligned} \quad (5)$$

$D_{np}$  corresponds to quasi-particle scattering operator,  $C_{np}^{\dagger}$  ( $C_{np}$ ) is a two quasi-particle creation (annihilation) operator for neutron-proton pair (for details see [34]). It satisfies the following bosonic commutation rules in the quasi-boson approximation.

$$[C_{np}, C_{np}^{\dagger}] \approx \delta_{nn'} \delta_{pp'}, \quad [C_{np}, C_{n'p'}] = 0 \quad (6)$$

Hence the effective Gamow-Teller (GT) interactions in the quasi-particle space can be written as follows (for details see [34]):

$$\begin{aligned} h_{ph}^{GT} &= h_{ph}^{CC} + h_{ph}^{DD} + h_{ph}^{CD} \\ h_{pp}^{GT} &= h_{pp}^{CC} + h_{pp}^{DD} + h_{pp}^{CD} \end{aligned} \quad (7)$$

Hamiltonian of the Gamow-Teller interaction in even-even nuclei and odd-odd nuclei and necessary formalism for deformed nuclei are given in detail in [34]. The effective interaction constants in the two channels were fixed from the experimental value of the GT resonance energy. Terms not commuting with GT operator were removed from the total Hamiltonian. The mean field approximation was renewed by adding an effective interaction term  $h_0$  [35] given as

$$h_0 = \sum_{\rho=\pm} \frac{1}{2\gamma_{\rho}} \sum_{\mu=0,\pm 1} [H_{sqp} - V_c - V_{ls} - V_1, G_{1\mu}^{\rho}]^{\dagger} [H_{sqp} - V_c - V_{ls} - V_1, G_{1\mu}^{\rho}]. \quad (8)$$

The strength parameter  $\gamma_{\rho}$  of the effective interaction was found from necessitating the commutation conditions (for details see [35, 36])

$$\gamma_{\rho} = \frac{\rho}{2} \langle 0 | [[H_{sqp} - V_c - V_{ls} - V_1, G_{1\mu}^{\rho}], G_{1\mu}^{\rho}] | 0 \rangle.$$

The GT operator  $G_{1\mu}^{\pm}$ , which commutes with the Hamiltonian, is given as

$$G_{1\mu}^{\pm} = \frac{1}{2} \sum_{k=1}^A [\sigma_{1\mu}(k) t_{+}(k) + \rho (-1)^{\mu} \sigma_{1-\mu}(k) t_{-}(k)] \quad (\rho = \pm 1), \quad (9)$$

where  $\sigma_{1\mu}(k) = 2s_{1\mu}(k)$  are the spherical components of the Pauli operators,  $t_{\pm} = t_x(k) \pm it_y(k)$  are the isospin raising/lowering operators.

The total Hamiltonian of Pyatov Method is

$$H_{PM} = H_{SQP} + h_0 + h_{ph} + h_{pp} \quad (10)$$

The GT transition strengths were calculated by summing the nuclear matrix elements

$$B_{GT}^{(\pm)}(\omega_i) = \sum_{\mu} \left| \mu_{\beta\pm}^i(0^+ \rightarrow 1^+) \right|^2, \quad (11)$$

where  $\omega_i$  are the excitation energies in the daughter nucleus. The  $\beta^{\pm}$  transition strengths were finally calculated using

$$B(GT)_{\pm} = \sum_i B_{GT}^{(\pm)}(\omega_i). \quad (12)$$

The calculated GT strengths should fulfill the Ikeda sum rule (ISR) [37]

$$ISR = B(GT)_{-} - B(GT)_{+} \cong 3(N - Z) \quad (13)$$

Calculated GT strength values from PM and SM can have differences because of the effective interaction term ( $h_0$ ) (for further details, see [9, 11, 34, 38,39]). Spherical calculations are done within the frame of Pyatov method and Schematic Model. In Pyatov Method, after symmetry deteriorations because of mean field approach restore by the help of efficient interaction  $h_0$ , beta decay interactions are taken into account in particle-hole and particle-particle channel. But, in Schematic Model, beta decay interactions are added without restored symmetry deteriorations [9, 11, 34, 38,39]).

### 3. Results and Discussions

The numerical calculations have been performed for the deformed nuclei and spherical nuclei in  $^{76}\text{Ge}$ . Nilsson single particle energies and wave functions have been calculated with a deformed Woods-Saxon potential [40]. The Gamow-Teller (GT) strength distributions,  $B(GT)$ . in Eq.(11) and sums  $B(GT)$ . in Eq.(12), for  $^{76}\text{Ge}$  within the SQP, SM and PM are calculated.  $^{76}\text{Ge}$  is chosen to reflect medium-heavy nuclei, which has experimental data on the GT strength distributions. It is discussed how to refine physical parameters related to this work.

#### 3.1. Deformation, particle-particle and particle-hole strength parameters and Ikeda sum rules in GT strength distributions

##### 3.1.1. Particle-particle and particle-hole parameters effect on GT distributions of deformed nuclei

In this section, it is wanted to see particle-hole and particle-particle parameters how effect on GT distributions of deformed nuclei. The deformed Woods-Saxon potential basis has been selected for a single particle basis. The issue has been solved within the framework of the proton-neutron quasi-particle random-phase approximation (QRPA), including the residual spin-isospin interaction between the nucleons in the particle-hole and particle-particle channels. The  $\beta_2$  deformation parameter of the corresponding nuclei in our calculation has been chosen from Moller et al. ( $\beta_2 = 0:143$ ) [41]. In single quasi-particle, interaction constants  $\chi_{ph}^{GT}$  and  $\chi_{pp}^{GT}$  don't affect to GT  $1^+$  states. That is why just Schematic model calculations are compared with other theoretical model and measured values.  $\chi_{ph}^{GT}$  values fixed,  $\chi_{pp}^{GT}$  values are changed in Fig.1;  $\chi_{pp}^{GT}$  value is fixed,  $\chi_{ph}^{GT}$  values are changed in Fig.2 to correspond to measured values. Here, particle-hole and particle-particle interaction parameters are calculated respectively with  $\chi_{ph}^{GT} = 5.2 A^{0.7}$  MeV and  $\chi_{pp}^{GT} = 0.58 A^{0.7}$  MeV and in figure 1 and 2, these parameters are fixed by multiplying the calculated values from the corresponding formula. In Fig.1, changes on the GT strength distributions for  $^{76}\text{Ge}$  for temporally fixed  $\chi_{pp} = 0.025, 0.0125$  and  $0$  with a fixed  $\chi_{ph}^{GT} = 5.2 A^{0.7}$  (0,25) MeV are observed. Deformed quasi-particle random-phase approximation (DQRPA)

calculated by E.Ha and Cheoun [27] is shown in the first column of Figures 1 and 2. E.Ha and Cheoun[27] fixed  $\mathcal{X}_{pp}=0, 0.5, \text{ and } 0.99$ , with a fixed  $\mathcal{X}_{ph}^{GT}=1.15$  to show the evolution of the GT strength distributions. The experimental data from the  $^{76}\text{Ge}(p, n)^{76}\text{As}$  reaction at 134.4 MeV is shown in the uppermost panel of Figs. 1 and 2 [29]. The calculated centroid from measured values is 9.84 MeV. The energy centroids which are calculated from the readings of drawn graphs by E.Ha and Cheoun [27] are found respectively 9.68, 10.64 and 11.42 MeV for  $\mathcal{X}_{pp}=0.99, 0.5$  and 0. The centroids in SM are found respectively 14.26, 14.76 and 15.07 for  $\mathcal{X}_{pp}=0.025, 0.0125$  and 0. Here, it is seen that the centroid has been shifted to higher energy as values of  $\mathcal{X}_{pp}$  falls for both models. Fig. 1 shows that when  $\mathcal{X}_{pp}$  is 0, GT fragmentation in SM is more than other calculation for different  $\mathcal{X}_{pp}$  values in SM while GT fragmentation in DQRPA is less than other calculation for different  $\mathcal{X}_{pp}$  values in DQRPA [27]. It is seen that the main peak of the first calculations in DQRPA is closer to the experimental one whereas the main peak of the third calculations in SM is closer to the experimental one. In general, it can be said that there is very little effect of pp interaction.

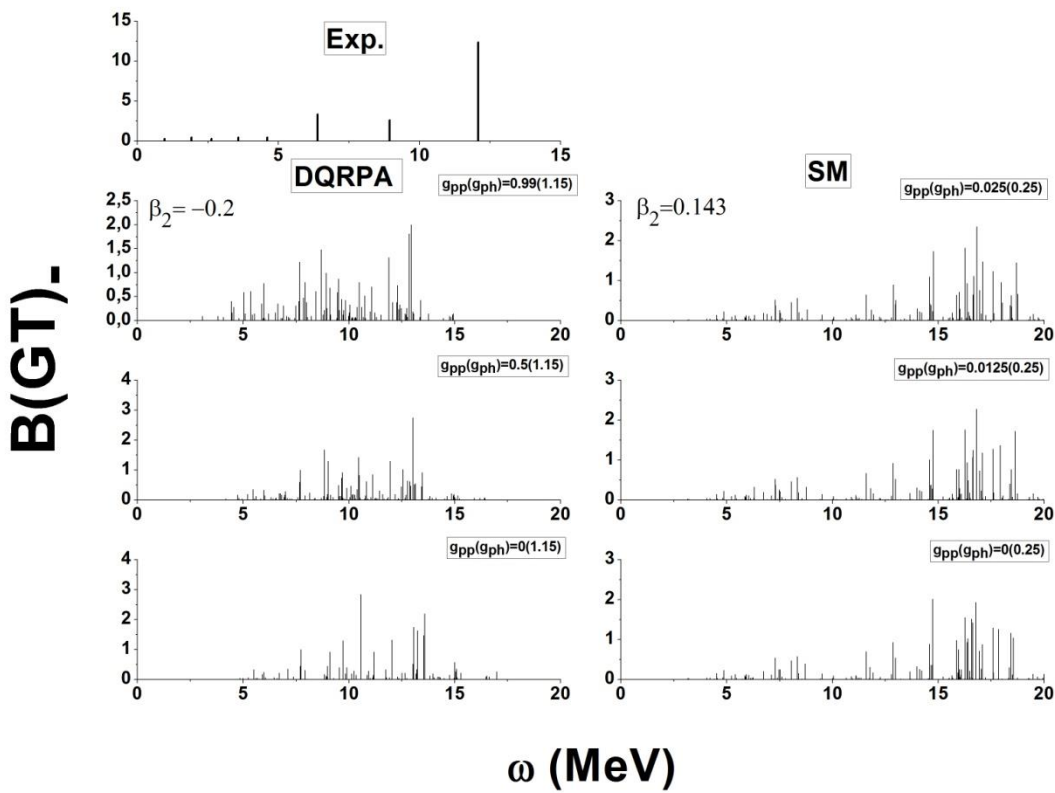


**Figure 1:** particle-particle parameters effect on the calculated B(GT). strength distributions in  $^{76}\text{Ge}$  compared with measured data and other theoretical model.

In Fig.2,  $\mathcal{X}_{pp}^{GT} = 0.58 A^{0.7}$  MeV is fixed in 0.0125 and  $\mathcal{X}_{ph}^{GT}$  is changed as respectively 0.025, 0.125 and 0.0625 to see changes of GT strength distributions. The GT strength distributions for  $^{76}\text{Ge}$  for a temporally fixed  $\beta_2 = -0.2$  are shown for different  $\mathcal{X}_{ph}=0, 0.5, \text{ and } 1.15$ , with a fixed  $\mathcal{X}_{pp}=0.99$  by E.Ha and Cheoun to comprehend the  $\mathcal{X}_{ph}$  dependence in Fig.2 [27]. The energy centroids, which are calculated from the readings of drawn graphs by E.Ha and Cheoun [27], are found respectively 9.66, 8.18 and 6.94 MeV for  $\mathcal{X}_{ph}=1.15, 0.5$  and 0. The centroids in SM are found respectively 14.26, 11.42 and 9.55 for  $\mathcal{X}_{ph}=0.25, 0.125$  and 0.0625. Here, it is seen that the centroid has been carried to lower energy as value of  $\mathcal{X}_{ph}$  falls for both models. But, there are not many changes in GT strength values. The centroid of the third graph in SM and the first graph in DQRPA is closer to measured centroid values.

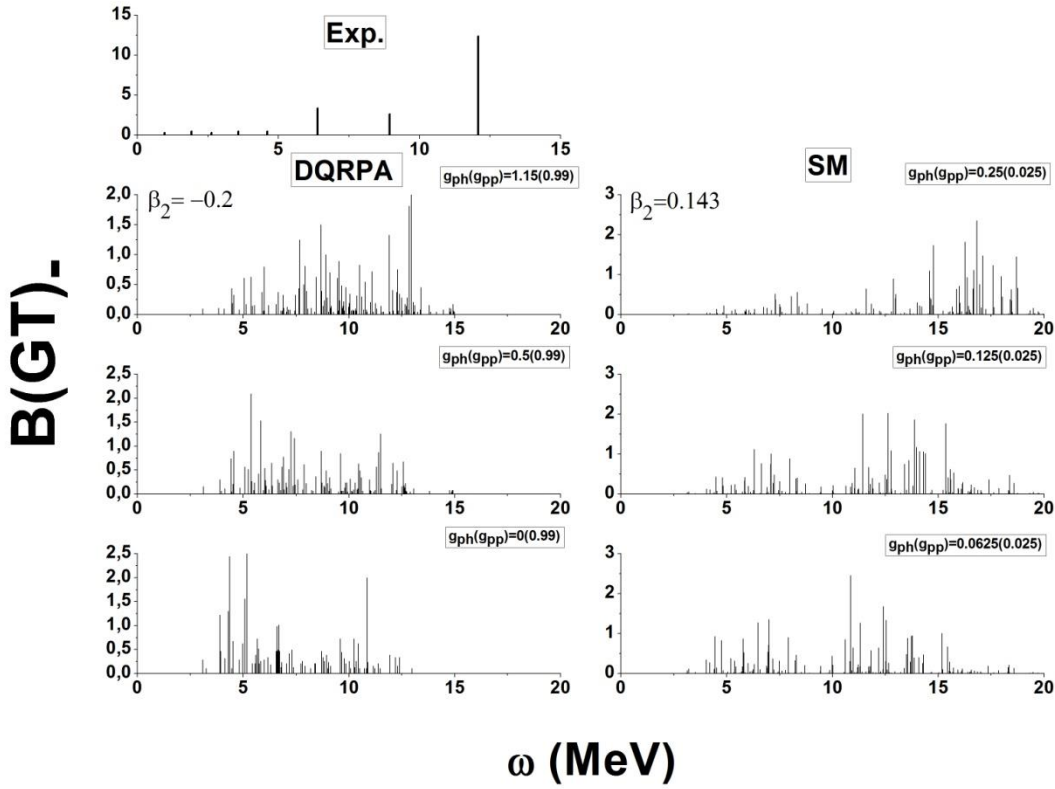


**Figure 2:** particle-hole parameters effect on the calculated B(GT). strength distributions in  $^{76}\text{Ge}$  compared with measured data and other theoretical model.

### 3.1.2. Deformation parameters

Figs. 3 and 4 have shown how effect on GT. strength distributions of  $^{76}\text{Ge}$  when deformation parameters are changed. Here, if the appropriate values for interaction constants  $\chi_{ph}^{GT}$  and  $\chi_{pp}^{GT}$  are chosen as  $\chi_{ph}^{GT} = 5.2 A^{0.7}$  MeV and  $\chi_{pp}^{GT} = 0.58 A^{0.7}$  MeV (0.125 and 0.025 MeV), it is possible to make the transition rate values closer to the experimental one as seen Figs 1 and 2. In the calculations, the following values for these constants have been fixed to see deformations affects on GT  $1^+$  states. The uppermost panels are the experimental data from the  $^{76}\text{Ge} (p, n)^{76}\text{As}$  reaction at 134.4 MeV, which show the main peak around 12 MeV in Figs 3 and 4 [29]. Fig. 3 shows GT strength distributions for  $\beta_2 = 0.1 - 0.3$ . The results of the DQRPA are displayed in the first column of Fig.3 for prolate shapes [27]. The second and third column of Fig.3 show respectively the results of Schematic Model (SM) and single quasi particle (SQP). It is seen from Fig.3 that the strong GT state peak in DQRPA for  $\beta_2 = 0.1-0.3$  is shifted from about 9 MeV to 12 MeV, the location of GT main peak in SM doesn't change and the strong GT state peak in SQP for  $\beta_2 = 0.1 - 0.3$  is shifted from about 10 MeV to 12 MeV. GT strength values in DQRPA and SQP are not changed when  $\beta_2$  is changed as a plus value. But the GT strength values are increased about 2-3 times when  $\beta_2$  is fixed as 0.3 in SM. GT  $1^+$  states are mainly populated within energy interval of 3-15 MeV in all models for  $\beta_2 = 0.1 - 0.3$ . All models strengths are well fragmented. The centroids calculated from E.Ha and Cheoun's calculation [27] are respectively 9.39, 9.46, 10.11 MeV for  $\beta_2 = 0.1-0.3$ . When the deformation parameter values are increased, the centroid is carried to the higher energies for DQRPA. For  $\beta_2 = 0.1-0.3$ , the centroids are respectively 11.76, 11.59 and 12.35 MeV for SM, 8.89, 8.82 and 9.55 for SQP. When deformation parameter is changed from  $\beta_2 = 0.1$  to  $\beta_2 = 0.2$ , the centroid is shifted the lower energy for both models. But, the centroid for  $\beta_2 = 0.3$  is at the higher energy for both models. Here it is noted that DQRPA, SM and SQP are in reasonable agreement with the low-lying measured data. This very good comparison with experimental data [29] can lead to a very reliable estimate of stellar weak rates using the SM.

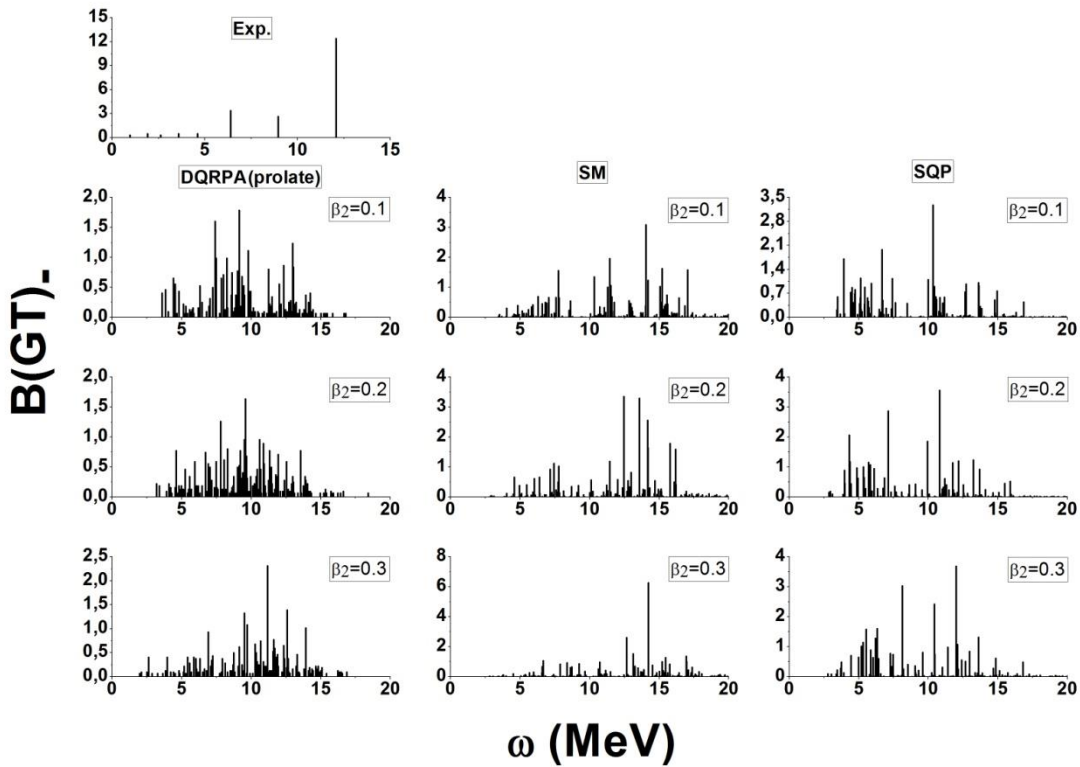


**Figure 3:** Deformation effects on the calculated B(GT)- strength distributions in  $^{76}\text{Ge}$  compared with measured data and other theoretical model.

GT. strength distribution for  $^{76}\text{Ge}$  is shown in Figure 4 for  $\beta_2 = (-0.1) - (-0.3)$ . The first column of Fig.4 shows the results of DQRPA for oblate shape [27]. Fig. 4 has presented that the location of the main peak in SM for  $\beta_2 = (-0.1) - (-0.3)$  doesn't change. But, the location of the strong GT state peak in DQRPA and SQP is not so noticeable changed when the deformation parameter is changed as a minus value. The main peak is located about 12 MeV in DQRPA and SQP and is in very good agreement with Exp. [29] it is noted that there is no visible change in GT strength values for all model when deformation parameter change as a minus value. GT  $1^+$  states are mainly populated within the energy interval of 3-15 MeV in all model. The centroids calculated from figures of [27] are obtained respectively 9.30, 9.84, 9.51 MeV for  $\beta_2 = (-0.1) - (-0.3)$ . For  $\beta_2 = (-0.1) - (-0.3)$ , the centroids are found respectively 10.94, 12.31 and 12.85 MeV for SM, 9.19, 9.66 and 8.97 for SQP. So, it shows that when the deformation parameter values are increased as minus value, the centroid is carried to the higher energies in SM. The centroid is shifted the higher energy for both DQRPA and SQP when deformation parameter is changed from  $\beta_2 = (-0.1)$  to  $\beta_2 = (-0.2)$ . But, the centroid for  $\beta_2 = (-0.3)$  is at the lower energy for both models.

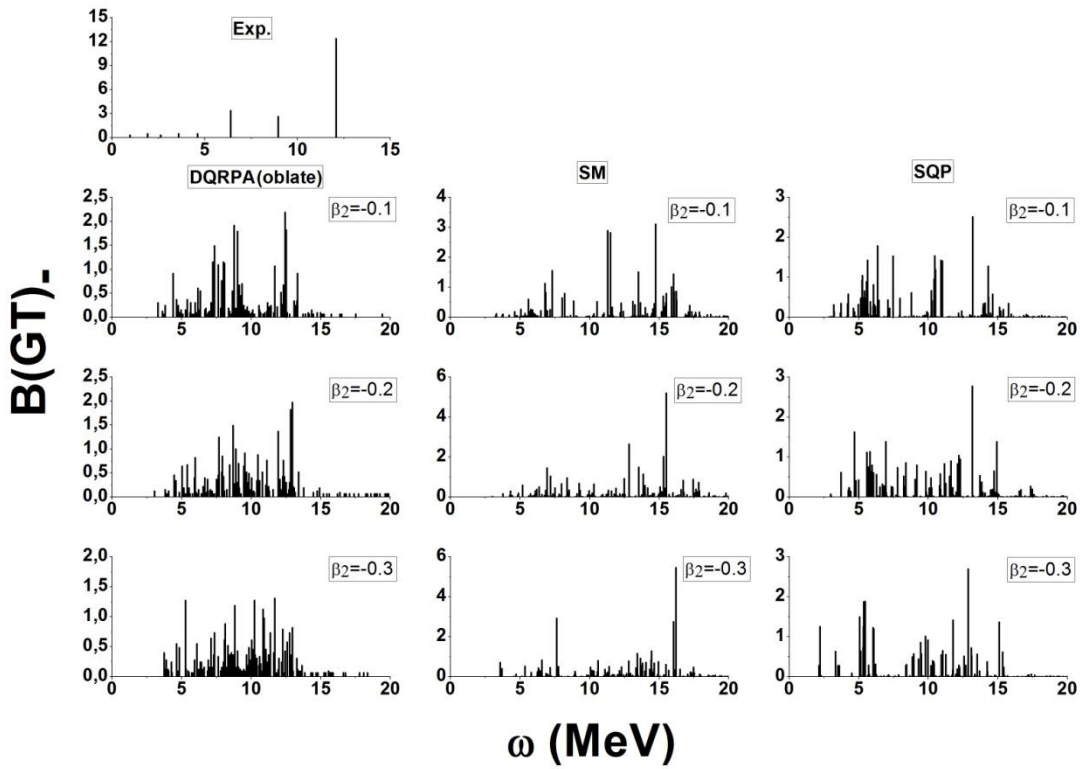


**Figure 4:** Deformation effects on the calculated B(GT)- strength distributions in  $^{76}\text{Ge}$  compared with measured data and other theoretical model.

### 3.1.3. Particle-particle and particle-hole parameters effect on GT distributions of spherical nuclei ( $\beta_2 = 0$ )

In this section, it will look that  $\chi_{ph}^{GT}$  and  $\chi_{pp}^{GT}$  effect on GT strength distribution for spherical nuclei (the deformation parameter is accepted as zero). In Figs 5 and 6, the results of Schematic Model (SM) and Pyatov Method (PM) are compared with the measured data. The uppermost panels are the experimental data from the  $^{76}\text{Ge}$  (p, n)  $^{76}\text{As}$  reaction at 134.4 MeV in Figs 5 and 6 [26]. In Fig. 5,  $\chi_{pp}^{GT}$  is fixed as 0.025 and  $\chi_{ph}^{GT}$  values are changed as  $2\chi_{ph}^{GT} = 5.2 A^{0.7}$  (0.5),  $\chi_{ph}^{GT} = 5.2 A^{0.7}$  (0.25) and  $\chi_{ph}^{GT} = 5.2 A^{0.7}$  (0.125) to see the effect of  $\chi_{ph}^{GT}$  on GT  $1^+$  distributions. The first column and the second column of Fig.5 show respectively the GT strength results of SM and PM. it is observed that the main peak is shifted to lower energies when  $\chi_{ph}^{GT}$  value is decreased for both SM and PM. For  $\chi_{ph}^{GT}=0.5, 0.25$  and  $0.125$ , the centroids are found respectively 16.42, 10.37 and 7.33 MeV in SM, 10.65, 4.68 and 2.81 MeV in PM. It is seen that the centroid value decreases when  $\chi_{ph}^{GT}$  value drops. Although, in SM, there is no visible change in GT strength value when  $\chi_{ph}^{GT}$  is altered; in PM,  $\chi_{ph}^{GT}$  reduces the value of GT strength. It is noted that the experimental result [29] is in very good agreement with the PM model calculation for  $\chi_{ph}^{GT}= 0.5$  and the SM model calculation for  $\chi_{ph}^{GT}= 0.25$ .

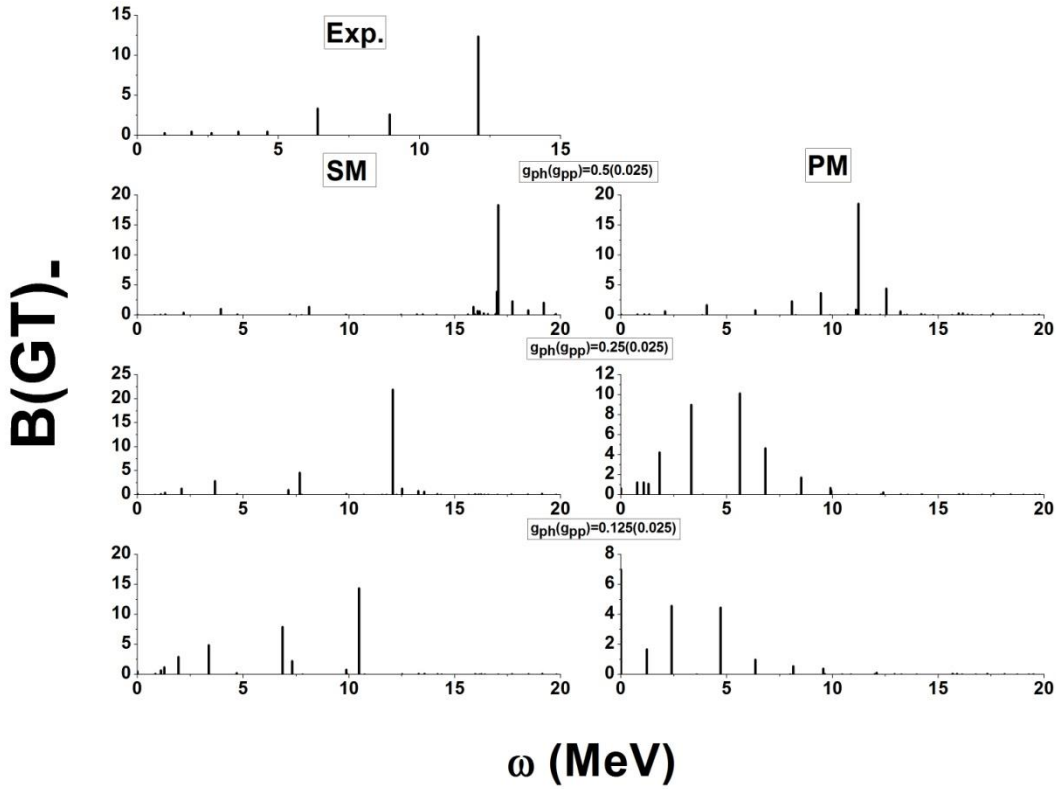


**Figure 5:** Effect of particle-hole parameters on the calculated B(GT). strength distributions in spherical  $^{76}\text{Ge}$  compared with measured data.

Figure 6 shows that  $\chi_{pp}^{GT}$  effects on the calculated B(GT). strength distributions in spherical  $^{76}\text{Ge}$  compared with measured data. In this figure,  $\chi_{ph}^{GT}$  is fixed as 0.25 in SM and 0.5 in PM to be compatible with the experiment [26].  $\chi_{pp}^{GT}$  is altered as  $\chi_{pp}^{GT} = 0.58 A^{0.7} (0.025)$ ,  $\chi_{pp}^{GT} = 0.58 A^{0.7} (0.0125)$  and 0 for both SM and PM to see how effects on GT distributions. The strong GT strength peak is located about 12 MeV for all  $\chi_{pp}^{GT}$  values in both models. There is no noticeable effect of  $\chi_{pp}^{GT}$  on GT strength distributions. The centroids are calculated as respectively 10.37, 10.74 and 11.09 MeV in SM; 10.65, 11.29 and 11.83 MeV in PM for  $\chi_{pp}^{GT}=0.025$ , 0.0125 and 0. It is noted that the centroid is shifted to higher energies when  $\chi_{pp}^{GT}$  value decreases. It can be seen from Fig. 6 that SM and PM results for all  $\chi_{pp}^{GT}$  values are in very good agreement with measured data. It can generally be said that experimental data is founded for spherical nuclei if the calculations for deformed nuclei are compared with the calculations for spherical nuclei. Because it can be seen that GT fragmentation in Exp. is more similar to the corresponding fragmentation in SM and PM for spherical nuclei (see Figs. 1-6). It can also be said that deformation led to more fragmentation of B(GT). strength.

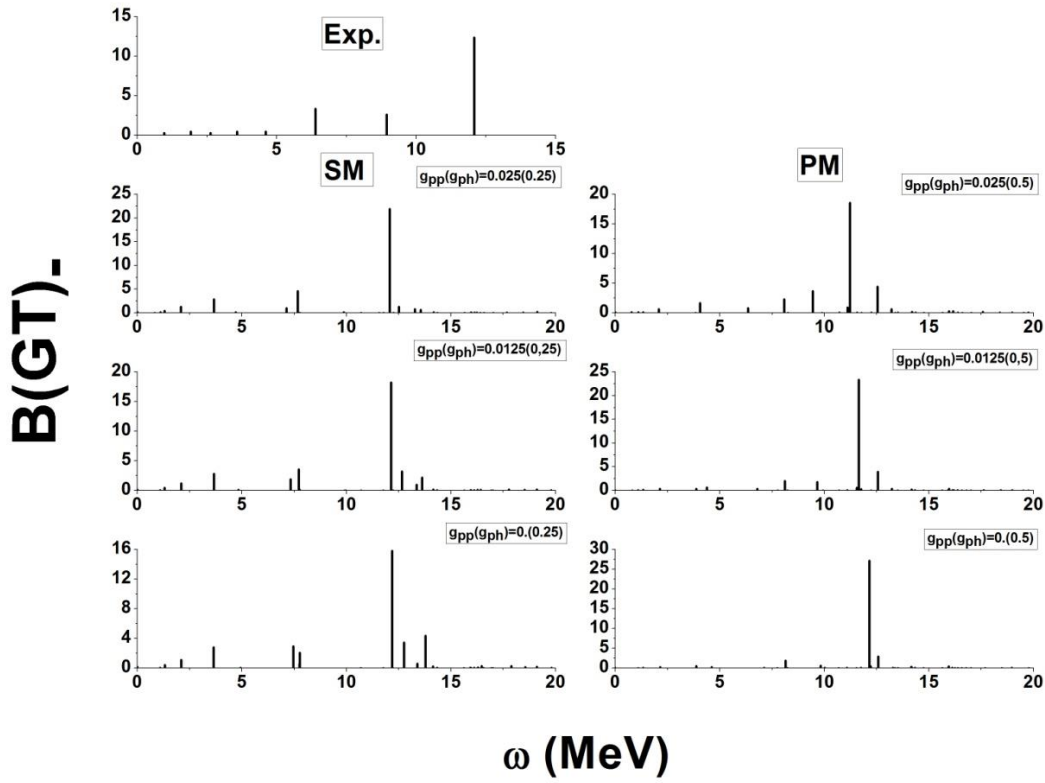


**Figure 6:** Effect of particle-particle parameters on the calculated B(GT)<sub>-</sub> strength distributions in spherical <sup>76</sup>Ge compared with measured data.

### 3.1.4. Ikeda sum rules

The calculated GT strengths should fulfill the Ikeda sum rule (ISR) [37]

$$ISR = B(GT)_{-} - B(GT)_{+} \cong 3(N - Z).$$

It is also wanted to check PM, SM and SQP models for <sup>76</sup>Ge perform when it comes to satisfying the model-independent Ikeda Sum Rule (ISR) (Eq. (13)). In Table 1, Ikeda Sum Rule values calculated for theoretical values are displayed for <sup>76</sup>Ge isotope. Here, there is no re-normalized in PM, SM, SQP and DQRPA [27]. Table 1 shows the percentage of providing the Ikeda sun rule. If the nucleons are treated as point particles and ignore two-body currents, the model-independent Ikeda sum rule should be satisfied by all calculations [37]. All model satisfy well (about %100) the sum rule for neutron-rich germanium isotope.

**Table 1:** Ikeda Sum for  $^{76}\text{Ge}$ .

3(N - Z) = 36		
Source	ISR	ISR (%)
$\chi_{ph}(\chi_{pp})=0.125(0.025)$		
$\beta_2 = 0.1$		
SQP	35.08	97.44
SM	35.38	98.28
$\beta_2 = 0.2$		
SQP	34.67	96.31
SM	34.03	94.53
$\beta_2 = 0.3$		
SQP	34.58	96.06
SM	35.84	99.56
$\beta_2 = -0.1$		
SQP	35.06	97.39
SM	38.81	92.19
$\beta_2 = -0.2$		
SQP	34.85	96.81
SM	36.14	99.61
$\beta_2 = -0.3$		
SQP	34.75	96.53
SM	36.52	98.56
$\chi_{ph}(\chi_{pp})=0.25(0.025)$		
$\beta_2 = 0$		
SQP	35.48	98.56
SM	35.48	98.56

### 3.2. Centroid and width values

The centroids and the widths of calculated GT strength distributions are calculated in all QRPA models for deformed and spherical nuclei in this section. Mathematically the GT centroid ( $\bar{E}_{\pm}$ ) can be calculated as:

$$\text{Centroid}(GT_{\pm}) = \frac{\sum_i E_i \times \Sigma B_i(GT_{\pm})}{\Sigma B_i(GT_{\pm})} \tag{14}$$

where  $E_i$  are the daughter excitation energies in units of MeV and  $B_i(GT_{\pm})$  are the corresponding calculated GT strength in  $\beta_+$  and  $\beta_-$  directions, respectively (in arbitrary units). The width of ( $GT_-$ ) is calculated by using the formula given below:

$$\text{Width}(GT_{\pm}) = \sqrt{\frac{\Sigma(E_i - \bar{E}_{\pm})^2 \times B_i(GT_{\pm})}{\Sigma B_i(GT_{\pm})}} \tag{15}$$

where  $\bar{E}_{\pm}$  are the centroids calculated as discussed above.

**Table 2:** Total B(GT) strength and width values along  $\beta$  directions for  $^{76}\text{Ge}$ .

Model	$\sum B(GT)_-$	Width <sub>-</sub>	Cut off Energy (MeV)
Exp	20.36	3.16	12.07
DQRPA [29]	37.49	2.85	16.80
SM(B)	36.29	3.81	54.95
PM(B)	35.65	3.04	54.89
SM(C)	39.89	4.05	47.82
sqp(C)	37.46	4.24	47.48

**Table 3:** Total B(GT) strength and centroid values along  $\beta$  directions for  $^{76}\text{Ge}$ .

Model	$\sum B(GT)_-$	$\bar{E}_-$ (MeV)	Cut off Energy (MeV)	
Exp	20.36	9.84	12.07	
DQRPA [29]	37.49	9.39	16.80	
pn-QRPA	16.30	8.66	26.50	
SM(B)	36.29	10.37	54.95	
PM(B)	35.65	10.65	54.89	
SM(C)	k=0	14.70	9.25	47.67
	k=1	25.19	9.70	47.82
	Total	39.89	9.55	47.82
sqp(C)	k=0	12.47	9.07	47.48
	k=1	24.98	8.81	47.48
	Total	37.45	8.89	47.48

Comparison of the centroids, the widths and the total B(GT) strength in the  $\beta$  direction with cut off energy is shown in Table 2 and 3. All three models classified into sub models are referred to as SM (B), PM (B), SM (C) and SQP (C) to see the effect of particle-hole (ph), particle-particle (pp) and deformation parameters on the centroid and the width. SM (B) and PM (B) show results of spherical SM and PM with both ph+pp channels ( $\beta_2 = 0$ ;  $\mathcal{X}_{ph}(\mathcal{X}_{pp}) = 0.25(0.025)$  for SM,  $\mathcal{X}_{ph}(\mathcal{X}_{pp}) = 0.5(0.025)$  for PM). SQP(C) and SM(C) are results of deformed SQP and SM with both ph+pp channels ( $\beta_2 = 0.143$  for SM,  $\beta_2 = 0.1$  for SQP ;  $\mathcal{X}_{ph}(\mathcal{X}_{pp}) = 0.0625(0.025)$ ). In Table 2, the  $^{76}\text{Ge}(p, n)^{76}\text{As}$  width data of 3.16 units calculated from [29] is in very good agreement with SM (B) and PM (B) values of 3.81 and 3.04 units. Although width calculated from graph of [27] is the smallest value in the other calculations and measured data, SM (C) and SQP (C) calculate the bigger width value than theoretical models and experiment. This shows that nuclear deformation has increased the width values in  $\beta$  direction.

The results are given for separately  $k = 0$  and  $k = 1$  of deformed SM and SQP in Table 3. It is seen that  $\sum B(GT)_-$  calculated by DQRPA ( $\beta_2 = 0.1$ ) [27] is very close to corresponding results calculated by SM and PM and SQP for spherical and deformed nuclei and it is the biggest value than pn-QRPA calculated by Jameel-Un Nabi and Mavra Ishfaq [28] and the experiment values [29]. Maybe the reason can be that the energy cut off in high energies in SM, PM and SQP. In the case of  $^{76}\text{Ge}$  the calculated total strength value of 16.30 units of pn-QRPA calculated by Jameel-Un Nabi and Mavra Ishfaq [28] is closer to the measured value of 20.36 units. Here one notes that whereas SM, PM and SQP models calculated bigger GT strength, they are the SQP (C) and SM (C) model in which the centroid of GT distributions resides at low excitation energy in daughter nucleus. This transforms into bigger weak-interaction rates

once the phase space functions are also incorporated. The SM and SQP calculated centroids of deformed nuclei are in excellent agreement with measured data. But, The SM and SQP calculated centroids of spherical nuclei are not much different from experiment value. It is seen from Table 3 that the nuclear deformation parameter has very little effect on total B(GT) and centroid in the  $\beta$  direction. It is noted that the SQP (C) and pn-QRPA [23] model place centroid at relatively low energies in daughter compared with other calculations. It can be also said that the centroid placement is also decent in all model when compared with experimental data.

#### 4. Summary and Conclusions

As it is known, Gamow-Teller transition has an important place in astrophysical events (for example; electron capture,  $\beta$ -decay, the supernova explosion, etc.) [1,2,3,4]. Because of this reason, in this study, it is aimed to examine the property of Gamow-Teller transition in the astrophysical circumstances and felt motivated to handled germanium isotopes which are fp shell nuclei. In this paper, Gamow-Teller transitions were studied by using Single Quasi Particle, Schematic Model and Pyatov Method in  $^{76}\text{Ge}$  isotope for the first time. Within this framework, the effects of particle-hole, particle-particle force and deformation are taken into account. The values of the centroids, the widths, ISR and total B(GT) in the  $\beta$ -decay directions are compared between the theoretical models and the measured data. At the same time, the calculated GT strength functions by using our models were compared with the corresponding experimental and other theoretical model calculations wherever available.

Firstly,  $\chi_{ph}^{GT}$  value is fixed,  $\chi_{pp}^{GT}$  value is changed. Secondly,  $\chi_{pp}^{GT}$  value is fixed,  $\chi_{ph}^{GT}$  value is changed to see particle-hole and particle-particle parameter how effect on GT distributions of deformed nuclei ( $\beta_2$  is fixed). As it was expected, it is seen that the centroid has been shifted to higher energy as value of  $\chi_{pp}^{GT}$  falls although the centroid has been carried to lower energy as the value of  $\chi_{ph}^{GT}$  falls. Then,  $\chi_{ph}^{GT}$  and  $\chi_{pp}^{GT}$  are fixed, the deformation parameter is changed to observe the deformation effects on GT  $1^+$  states. It is seen that DQRPA [27], SM and SQP are in reasonable agreement with the low-lying measured data. This very good comparison with experimental data can lead to a very reliable estimate of stellar weak rates using the SM. It can also be said that deformation led to more fragmentation of B(GT) strength. Finally, the deformation parameter is accepted as zero and  $\chi_{ph}^{GT}$  and  $\chi_{pp}^{GT}$  are changed because of looking to effect on GT strength distribution for spherical nuclei. The main peak is shifted to lower energies when  $\chi_{ph}^{GT}$  value is decreased for both SM and PM and also, the centroid value decreases when  $\chi_{ph}^{GT}$  value drops. The centroid is shifted to higher energies when  $\chi_{pp}^{GT}$  value decreases. SM and PM result values are in very good agreement with measured data. It can generally be said that experimental data is founded for spherical nuclei if the calculations for deformed nuclei are compared with the calculations for spherical nuclei.

Our calculations showed that the models with deformation of the nucleus incorporated gave better results for total GT strength and fulfillment of Ikeda sum rule as against those models performed in spherical basis. Not only the model results were in good agreement with measured data but it also resulted in placement of centroid at low excitation energies. It was also concluded that GT centroid the placement by the SQP, SM and PM models is, in general, in very good agreement with the centroids of measured data and also the  $^{76}\text{Ge}(p, n)^{76}\text{As}$  width data [29] of 3.16 units is in very good agreement with SM (B) and PM (B) values of 3.81 and 3.04 units.

One needs to microscopic and confidential calculation of GT strength distributions for hundreds of iron-regime nuclei for astrophysical applications. An important advance in our understanding of supernova explosions and heavy element nucleosynthesis to develop out of next-generation radioactive ion-beam facilities is assumed once measured GT strength distribution of many more nuclei (including unstable isotopes) is gotten. The calculating GT strength functions for other key fp-shell nuclei (including many neutron-rich unstable nuclei) are been studying and it is hoped that our findings will be presented in the near future.

**Acknowledgments:** I would like to acknowledge the support of the research grant provided by the BAP Project No. 2018-2117.

## References

- [1] Fuller G.M., Fowler W.A. and Newman M.J., Stellar weak-interaction rates for sd-shell nuclei. I. Nuclear matrix element systematics with application to  $^{26}\text{Al}$  and selected nuclei of importance to the supernova problem, *Astrophys. J. Suppl. Ser.*, 42 (1980) 447-473
- [2] Aufderheide M.B., Fushiki I., Woosley S.E., Stanford E. and Hartmann D.H., Search for important weak interaction nuclei in presupernova evolution, *Astrophys. J. Suppl. Ser.*, 91 (1994) 389–417.
- [3] Nabi J.-Un., Klapdor-Kleingrothaus H.V., Microscopic calculations of weak interaction rates of nuclei in stellar environment for  $A = 18$  to 100, *Eur. Phys. J. A*, 5 (1999) 337–339.
- [4] Langanke K., Martínez-Pinedo G., Shell-model calculations of stellar weak interaction rates. II. Weak rates for nuclei in the mass range  $A = 45$ –65 in supernovae environments, *Nucl. Phys. A*, 673 (2000) 481-508.
- [5] Pyatov N.I., Salamov D.I., Conservation laws and collective excitations in nuclei, *Nucleonica*, 22 (1977) 1–127.
- [6] Civitarese O., Hess P.D., Hirsch J.G. and Reboiro M., Spontaneous and dynamical breaking of mean field symmetries in the proton neutron quasi particle random phase approximation, *Phys. Rev. C*, 59 (1998) 194–199.
- [7] Magierski P., Wyss R., Self consistent effective interactions and symmetry restoration, *Phys. Lett. B*, 468 (2000) 54-60.
- [8] Kulliev A.A., Akkaya R., Ilhan M., Guliev E., Salamov C., Selvi S., Rotational invariant model of the states with  $K^\pi = 1^+$  and their contribution to the scissors mode, *Int. J. Mod. Phys. E*, 9 (2000) 249-261.
- [9] Babacan T., Salamov D.I., Kucukbursa A., Gamow–Teller  $1^+$  states in  $^{208}\text{Bi}$ , *Phys. Rev. C*, 71 (2005) 037303.
- [10] Babacan T., Salamov D.I., Kucukbursa A., The effect of the pairing interaction on the energies of isobar resonance in  $^{112-124}\text{Sb}$  and isospin admixture in  $^{100-124}\text{Sn}$  isotopes, *J. Phys. G*, 30 (2004) 759–770.
- [11] Babacan T., Salamov D.I., Kucukbursa A., The investigation of the  $\log(ft)$  values for the allowed Gamow–Teller transitions of some deformed nuclei, *Math. Comput. Appl.*, 10 (2005) 359–368.
- [12] Çakmak, N. The study of Charge Exchange collective Excitations in Odd mass nuclei, *Ph.D thesis.* (2008) 1-72.
- [13] Cole A.L., Akimune H., Austin Sam M., Bazin D., van den Berg A.M., Berg G.P.A., Brown J., Daito I., Fujita Y., Fujiwara M., Gupta S., Hara K., Harakeh M.N., Janecte J., Kawabata T., Nakamura T., Roberts D.A., Sherrill B.M., Steiner M., Ueno H., Zegers R.G.T., Measurement of the Gamow–Teller strength distribution in  $^{58}\text{Co}$  via the  $^{58}\text{Ni}(t, ^3\text{He})$  reaction at 115 MeV/nucleon, *Phys. Rev. C*, 74 (2006) 034333.
- [14] Fujita Y., et al., Gamow-Teller transitions from  $^{58}\text{Ni}$  to discrete states of  $^{58}\text{Cu}$ , *Eur. Phys. J. A*, 13 (2002) 411-418.
- [15] Fujita Y., et al., Isospin structure of  $J^\pi=1^+$  states in  $^{58}\text{Ni}$  and  $^{58}\text{Cu}$  studied by  $^{58}\text{Ni}(p,p')$  and  $^{58}\text{Ni}(^3\text{He},t)^{58}\text{Cu}$  measurements, *Phys. Rev. C*, 75 (2007) 034310.
- [16] El-Kateb S., Alford W.P., Abegg R., Azuma R.E., Brown B.A., Celler A., Frekers D., Häusser O., Helmer R., Henderson R.S., Hicks K.H., Jeppesen R., King J.D., Raywood K., Shut, G.G., Spicer B.M., Trudel A., Vetterli M., Yen, S., Spinisospin strength distributions for fp shell nuclei: results for the  $^{55}\text{Mn}(n,p)$ ,  $^{56}\text{Fe}(n,p)$ , and  $^{58}\text{Ni}(n,p)$  reactions at 198 MeV, *Phys. Rev. C*, 49 (1994) 3128.
- [17] Sasano M., et al., Gamow-Teller Transition Strengths from  $^{56}\text{Ni}$ , *Phys. Rev. Lett.*, 107 (2011) 202501.
- [18] Poves A., Snchez-Solano J., Caurier E., Nowacki F., Shell model study of the isobaric chains  $A = 50$ ,  $A = 51$  and  $A = 52$ , *Nucl. Phys. A*, 694 (2001)157–198.
- [19] Richter W.A., Merwe M.G., Van Der Julies R.E., Brown B.A., New effective interactions for the  $0f$   $1_p$  shell, *Nucl. Phys. A*, 253 (1991) 325–353.
- [20] Suzuki T., Honma M., Higashiyama K., Yoshida T., Kajino T., Otsuka T., Umeda H., Nomoto K., Neutrino-induced reactions on  $^{56}\text{Fe}$  and  $^{56}\text{Ni}$ , and production of  $^{55}\text{Mn}$  in population III stars, *Phys. Rev. C*, 79 (2009)

061603.

- [21] Caurier C., Langanke K., Martinez-Pinedo G., Nowacki F., Shell-model calculations of stellar weak interaction rates. I. Gamow-Teller distributions and spectra of nuclei in the mass range  $A = 45-65$ , *Nucl. Phys. A*, 653 (1999) 439-452.
- [22] Sarriguren P., Moya de Guerra E., Alvarez-Rodriguez R., Gamow-Teller strength distributions in Fe and Ni, *Nucl. Phys. A*, 716 (2003) 230-244.
- [23] Nabi, J.-Un., Klapdor-Kleingrothaus, H.V., Microscopic calculations of stellar weak interaction rates and energy losses for fp- and fpghshell nuclei, *At. Data Nucl. Data Tables*, 88 (2004) 237-476.
- [24] Nabi, J.-Un., Klapdor-Kleingrothaus, H.V., 1999. Weak interaction rates of sd-shell nuclei in stellar environments calculated in the protonneutron quasiparticle random-phase approximation, *At. Data Nucl. Data Tables*, 71 (1999) 149-335.
- [25] Ha Eunja, Cheoun Myung- Ki and Kim K.S., Deformation effects on the Gamow-teller transitions in  $^{76}\text{Ge}$  and  $^{76}\text{Se}$  by using the deformed Quasi-Particle Random-Phase Approximation, *Journal of the Korean Physical Society*, 67 (2015) 1142-1149.
- [26] Sarriguren P., et al., Gamow-Teller strength distributions in  $^{76}\text{Ge}$  and  $^{76}\text{Se}$  from deformed quasiparticle random-phase approximation, *Phys. Rev. C*, 67 (2003) 044313.
- [27] Ha Eunja and Cheoun Myung-Ki, Gamow-Teller strength distributions in  $^{76}\text{Ge}$ ,  $^{76,82}\text{Se}$ , and  $^{90,92}\text{Zr}$  by the deformed proton-neutron QRPA, *Nuclear Physics A*, 934 (2015) 73-109.
- [28] Nabi Jameel-Un and Ishfaq Mavra, Gamow-Teller strength distributions and stellar weak-interaction rates for  $^{76}\text{Ge}$  and  $^{82}\text{Se}$  using the deformed pn-QRPA model, *Astrophys. and Space Sci.*, 361, (2016) 1-10.
- [29] Madey R., Flanders B.S., Anderson B.D., Baldwin A.R., Watson J.W., Low-lying structures in the Gamow-Teller strength functions for the double-beta-decaying nuclei  $^{76}\text{Ge}$ ,  $^{82}\text{Se}$ ,  $^{128}\text{Te}$ , and  $^{130}\text{Te}$ , *Phys. Rev. C*, 40 (1989) 540-552.
- [30] Sarriguren P., Moya de Guerra E., Escuderos A., and Carrizo A.C.,  $\beta$  decay and shape isomerism in  $^{74}\text{Kr}$ , *Nucl. Phys. A*, 635 (1998) 55-85.
- [31] Raman S., Nestor C. W., Tikkanen Jr. and P., Transition Probability from the Ground to the First-Excited  $2^+$  State of Even-Even Nuclides, *At. Data Nucl. Data Tables*, 78 (2001) 1-128.
- [32] Simkovic F., Pacearescu L. and Faessler A., Two-neutrino double beta decay of  $^{76}\text{Ge}$  within deformed QRPA, *Nucl. Phys. A*, 733 (2004) 321-350.
- [33] Yousef M. S., Rodin V., Faessler A. and Simkovic F., Two-neutrino double  $\beta$  decay of deformed nuclei within the quasiparticle random-phase approximation with a realistic interaction, *Phys. Rev. C*, 79 (2009) 014314.
- [34] Salamov D.I., Kucukbursa A., Maras I., Aygor H.A., Babacan T., Bircan H., Calculation of the  $\log(ft)$  values for the allowed Gamow-Teller transitions in deformed nuclei using the basis of Woods-Saxon wave functions, *Acta Phys. Slov.* 53 (2003) 307-319.
- [35] Cakmak, S., Nabi, J.-U., Babacan, T., Selam, C., Study of Gamow-Teller transitions in isotopes of titanium within the quasi particle random phase approximation, *Astrophys. Space Sci.*, 352 (2014) 645-663.
- [36] Salamov, D.I. et al., Proceedings of Fifth Conference on Nuclear and Particle Physics (NUPPAC 05), vol. 361, Cairo, August 2006.
- [37] Ikeda, K.I., Collective Excitation of Unlike Pair States in Heavier Nuclei. *Prog. Theor. Phys.*, 31 (1964) 434-451.
- [38] Cakmak, N., Unlu, S., Selam, C., Gamow-Teller  $1^+$  states in  $^{112-124}\text{Sb}$  isotopes, *Pramana J. Phys*, 75 (2010) 649-663.
- [39] Selam, C., Babacan, T., Bircan, H., Aygor, H.A., Kucukbursa, A., Maras, I., The investigation of the  $\log(ft)$  values for the allowed Gamow-Teller transitions of some deformed nuclei, *Math. Comput. Appl.*, 9 (2004) 79-90.
- [40] Cerkaski M., Dudek J., Szymanski Z., Andersson C. G., Leander G., Aberg S., Nilsson S. G. and Ragnarsson I., Search for the yrast traps in neutron deficient rare earth nuclei, *Phys. Lett. B*, 70 (1977) 9-13; Dudek J.,

Nazarewicz W., Faessler A., Theoretical analysis of the single-particle states in the secondary minima of fissioning nuclei, *Nucl. Phys. A*, 412 (1984) 61-91.

[41] Moller P., et al., Nuclear Ground-State Masses and Deformations, *Atomic Data and Nuclear Tables*, 59 (1995) 185-381.